Desalination and Water Treatment
www.deswater.com

doi: 10.1080/19443994.2014.880658

54 (2015) 332–341
April

Taylor & Francis
Taylor & Francis Group

Kinetics and mechanism of sorption of chloride ion from sodium carbonate manufacturing wastewater by Mg–Al oxide

Roya Hamidi[a], Pezhman Kazemi[b,*]

[a]*Water and Sustainable Development, Institute of Environmental Engineering, Sahand University of Technology, Tabriz, Iran*
[b]*Department of Chemical Engineering, Islamic Azad University, South Tehran Branch, Tehran, Iran*
Tel. +98 2634437364; email: Pezhman.kazemi@gmail.com

Received 3 August 2013; Accepted 31 December 2013

ABSTRACT

In this article, the removal of chloride ion generated from industrial wastewater was examined by using magnesium–aluminum (Mg–Al) oxide obtained from Mg–Al layered double hydroxide. The influences of conditions for chloride ion uptake, including quantity of Mg–Al oxide, contact time and temperature on anion exchange has been investigated, respectively. The extent of the chloride, ion removal increased with an increase in the quantity of Mg–Al oxide, contact time, and temperature. Thermodynamic parameters including Gibbs free energy (ΔG°), standard enthalpy change (ΔH°), and standard entropy change (ΔS°) for the process were calculated using the Langmuir constants. Kinetic analyses were conducted using pseudo-first and second-order models. The regression results showed that the uptake process was more accurately represented by pseudo-second-order model. The calculated value of E_a was found to be 77.428 kJ/mol, which indicate that the process of uptake of chloride ion is controlled by the rate of reaction of chloride ion with the Mg–Al oxide rather than diffusion. Results suggested that the uptake process was feasible and endothermic.

Keywords: Layered double hydroxide; Chloride; Anion exchange; Thermodynamic; Isotherm

1. Introduction

Production of industrial wastewater from different industries and allowing them to enter the environment have been considered in recent years. Increased awareness of pollution and its effects has emphasized the importance of water quality management. Effective water quality management requires that the concentrations and effects of pollutants can be accurately assessed, and the consequences of proposed discharges can be predicted. The source of wastewater containing chloride ion is extensive, discharging from such as landfill, tanning, pickling, seafood canning, and sodium carbonate manufacturing industries. The high salt content in the wastewaters could cause the corrosion of waste pipe or the agricultural wreck of crops by damage from salt [1–7]. Therefore, it should be required that undesirable pollution is removed.

One of the wastewaters with high containing of chloride ion is sodium carbonate manufacturing industries. Distiller waste (DW) is the main waste materials that are formed during the Solvay process

---

*Corresponding author.

[8–10]. In most cases to disposing of DW, this suspension is directed to sedimentation ponds, where solid particles are settled. Then the cleared overflow of DW is directed as sewage to the nearest ambient such as river, sea, etc. This may lead to an increase in both pH and chloride ion concentration in the ambient, especially near areas to sodium carbonate plant [11]. So, it is considered that this method is not appropriate and to complete the treatment, wastewater must be treated at public wastewater treatment plants such as sewage-works.

Layered double hydroxides (LDHs), also known as hydrotalcite-like compounds (HTs), have been extensively studied to demonstrate their reactivity toward hazardous anionic contaminants, which is due to their high anion exchange capacity and large surface area. These materials have a general chemical formula $[Mg^{2+}{}_{1-x}Al^{3+}{}_{x}(OH)_2](A^{n-})_{x/n}\cdot mH_2O$, where x denotes the Al/(Mg + Al) molar ratio ($0.20 \leq x \leq 0.33$) and A^{n-} is an anion such as $CO_3{}^{2-}$ or Cl^- [12,13]. Furthermore, Mg–Al LDH intercalated with $CO_3{}^{2-}$ (CO_3•Mg–Al LDH), can be converted into Mg–Al oxide by calcination at 450–800°C, as expressed by Eq. (1) [14–16]:

$$Mg_{1-x}Al_x(OH)_2(CO_3)_{x/2} \rightarrow Mg_{1-x}Al_xO_{1+x/2} + x/2CO_2 + H_2O \quad (1)$$

The Mg–Al oxide can in turn intercalate anions in solution, reconstructing the HT structure, as shown in Eq. (2) [14–16]:

$$Mg_{1-x}Al_xO_{1+x/2} + x/nA^{n-} + (1 + x/2)H_2O \rightarrow Mg_{1-x}Al_x(OH)_2A_{x/n} + xOH^- \quad (2)$$

Eq. (2) indicates that the rehydration and subsequent combination of Mg–Al oxide with anions in solution is accompanied by the release of OH^-.

Previous studies have demonstrated the reactivity of Mg–Al oxide toward several contaminants, such as color [17], fluoride [18], trichlorophenol [19], benzoate [20,21], phosphate [22,23], chromate [24–26], chloride [2–5,27–31], antimonate [32], and arsenite [33]. Although, previous studies have revealed the promising performance of Mg–Al oxide in removing anionic contaminants from water under laboratory conditions, some uncertainties exist with respect to the removal efficiency of Mg–Al oxide in real-world conditions. Industrial wastewater and contaminated surface water and groundwater usually have a chemical composition much more complex than those used in laboratory studies.

In this study, Mg–Al oxide was applied and evaluated as a possible ion exchangers/adsorbents for the removal of chloride ion from real wastewater contained multicomponents of $CaCl_2$, NaCl, and $MgCl_2$ solutions. The aim of this study is to investigate the effect of the quantity of Mg–Al oxide, temperature, and contact time on the removal operation. Kinetics and thermodynamics studies have been done and the results have been analyzed by applying conventional theoretical methods. Thermodynamic parameters, such as ΔG°, ΔH°, and ΔS°, were calculated.

2. Experimental

2.1. Materials

All the chemicals used were obtained from Merck Company (Frankfurt, Germany). The wastewater was obtained from DW of Kaveh Soda Sodium Carbonate Manufacturing Company (Maragheh, Iran). The chemical composition of this wastewater is shown in Table 1. According to this composition and using the bar diagram, the predicted compounds of DW was obtained as shown in Table 2.

2.2. Preparation of Mg–Al oxide

The synthesis of CO_3-HTs was conducted using a constant-pH co-precipitation method [34–36]. $Mg(NO_3)_2$ and $Al(NO_3)_3$ solutions with Mg/Al molar ratio of 4.0 were added to 1.0 M Na_2CO_3 solution. The resulting solutions were kept at a pH of 10.0 by adding a solution of 2.0 M NaOH. After stirring, obtained

Table 1
Wastewater chemical composition

Ions	Unit	
Calcium	mg $CaCO_3$/L	110,775
Magnesium	mg $CaCO_3$/L	5,800
Sodium	mg/L	20,050
Chloride	mg/L	99,400
Sulfate	mg/L	2,579

Table 2
Components of DW

Element	Concentration (kg/m^3)
$Ca(HCO_3)_2$	20.250
$CaSO_4$	7.31
$MgCl_2$	9.70
$CaCl_2$	98.86
Nacl	48.22

slurry was heated at 40℃ for 4 h and then be taken at 70℃ for 40 h under stirring. The resulting precipitate was then isolated by filtration and washing with deionized water until NO_3^- ions were vanished from the filtrate. The sample was dried at 105℃ for 24 h. The chemical composition of the CO_3^{2-}-HT was $Mg_{0.80}Al_{0.20}(OH)_2(CO_3)_{0.10}.0.78H_2O$. Mg–Al oxide was prepared by calcining the prepared CO_3^{2-}-HT at 500℃ for 1 h with chemical composition of $Mg_{0.80}Al_{0.20}O_{1.10}$.

2.3. Characterization

X-ray diffraction (XRD) was carried out using Cu-Kα radiation in a USA made Bruker AXS D8-ADVANCE instrument at a step size of 0.05° scanned for 1s. The morphological feature of the powder was examined by a Hitachi S-4160 field emission scan electron microanalyser (FESEM). The specific surface area of the $Mg_{0.80}Al_{0.20}O_{1.10}$ was measured by BET N_2-adsorption method at 77 K using a Chem BET 3000 device.

2.4. Removal of chloride ion

The effect of adsorbent dosage on removing cl ion from wastewater was studied by using 100 mL of the considered wastewater solution in conjuction with 0.5, 1, 1.5, and 2 times of stoichiometric amount, which was equal to 59, 118, 177, and 236 gr/L according to Eqs. (3)–(5) [3,27,28]. Samples were collected at 5, 15, 30, 45, 90, and 120 min to determine the optimum values of contact time. Isotherm experiment were carried out at 99,400 mg/L as initial cl concentration and optimum Mg–Al oxide dosage and contact time. Other adsorption experiments were also done at 30, 45, and 60℃ to determine the effect of temperature on the adsorption process and to evaluate the adsorption thermodynamic parameters.

$$\begin{aligned}&Mg_{0.8}Al_{0.2}O_{1.1} + 0.2NaCl + 1.1H_2O\\&\rightarrow Mg_{0.8}Al_{0.2}(OH)_2Cl_{0.2} + 0.2NaOH\end{aligned} \tag{3}$$

$$\begin{aligned}&Mg_{0.8}Al_{0.2}O_{1.1} + 0.1MgCl_2 + 1.1H_2O\\&\rightarrow Mg_{0.8}Al_{0.2}(OH)_2Cl_{0.2} + 0.1Mg(OH)_2\end{aligned} \tag{4}$$

$$\begin{aligned}&Mg_{0.8}Al_{0.2}O_{1.1} + 0.1CaCl_2 + 1.1H_2O\\&\rightarrow Mg_{0.8}Al_{0.2}(OH)_2Cl_{0.2} + 0.1Ca(OH)_2\end{aligned} \tag{5}$$

The suspended solutions were filtrated and analyzed for ions concentration values. For this purpose, the chloride concentration of the filtrate was determined by argentometric method using potassium chromate as an indicator [6].

The percentage removal of chloride ion and the chloride ion loading (in mg per unit mass of Mg–Al oxide, q_e), was obtained by the following equations:

$$\text{Removal}\,\% = \frac{C_0 - C_e}{C_0} \times 100 \tag{6}$$

$$q_e = \frac{(C_0 - C_e)V}{m} \tag{7}$$

where C_0 (mg/L) and C_e (mg/L) are initial and equilibrium chloride concentrations, respectively, V (L) is the initial volume of solution, and m (g) is the mass of Mg–Al oxide.

Kinetic experiments were made by dispersing $Mg_{0.80}A_{l0.20}O_{1.10}$ samples in 100 mL of chloride solutions with an initial concentration of 99,400 mg/L and stirred for selected time intervals. Chloride ion uptake by the $Mg_{0.80}Al_{0.20}O_{1.10}$ was calculated according to Eq. (8):

$$q_t = \frac{(C_0 - C_t)V}{m} \tag{8}$$

where q_t (mg/g) is the uptake capacity of chloride by $Mg_{0.80}Al_{0.20}O_{1.10}$ at time t, V (L) is the volume of solution, C_0 (mg/L) and C_t (mg/L) are initial chloride concentration and chloride concentration at time t, and m (g) is the mass of $Mg_{0.80}Al_{0.20}O_{1.10}$.

3. Results and discussion

3.1. Characterization of Mg–Al oxide

Fig. 1 shows the XRD patterns of $Mg_{0.80}Al_{0.20}(OH)_2(CO_3)_{0.10}.0.78H_2O$ and $Mg_{0.80}Al_{0.20}O_{1.10}$. It can be seen that the sharp and symmetric peaks at lower 2θ values are characteristic of HTs. The positions of direction lines correspond to the (0 0 1) at low values of 2θ angles and (1 1 0), (1 1 3) reflections at higher values of 2θ [34]. As seen, all the XRD peaks of $Mg_{0.80}Al_{0.20}(OH)_2(CO_3)_{0.10}.0.78H_2O$ correspond to those of HT (JCPDS card 22–700) and the prepared CO_3^{2-}-HT confirm to have the structure of HT. The XRD pattern of HT is generally indexed based on hexagonal unit cell, with a base spacing equivalent to $1/n$ of c parameter where n is the layer repeat of the unit cell [28,35]. Whereas, the parameter c corresponds to three times distance between adjacent brucite-like layers, which can be determined from the equation $c = 3\{d(003) + 2d(006)\}/2$ [37]. The positions of diffraction lines of $Mg_{0.80}Al_{0.20}O_{1.10}$ corresponded to the (2 0 0) and (2 2 0)

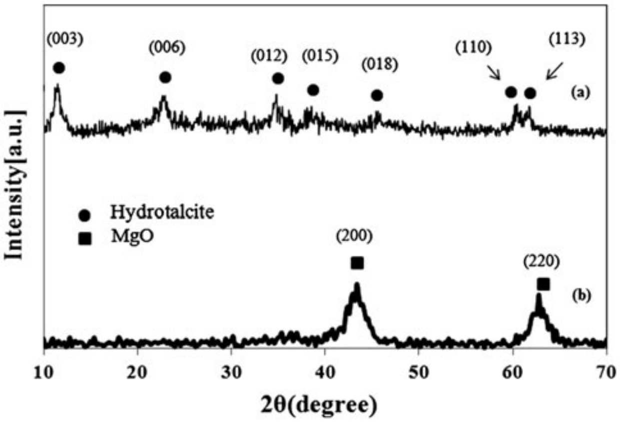

Fig. 1. XRD patterns of (a) $Mg_{0.80}Al_{0.20}(OH)_2(CO_3)_{0.10} \cdot 0.78H_2O$ and (b) $Mg_{0.80}Al_{0.20}O_{1.10}$.

diffraction of mixed cubic MgO oxide (JCPDS card 4-829) [34]. FESEM is used to measure particle size and to observe the direct agglomeration of the particle. Fig. 2 shows morphology of the Mg–Al oxide. The surface morphology reveals spherical particles of close size, coexisting with agglomerate. The particle size of Mg–Al oxide estimated by the FESEM image was in the nanometer range. Nanoparticle can be bonded together by two kinds of mechanisms-aggregation and agglomeration. Aggregation refers to the sintering together of particles; and agglomeration refers to adhesion of particles to each other because of attractions such as Van der Waals forces. One of the main advantages of the HT derived mixed Mg–Al oxides is a high surface area. The BET specific surface area of the mixed oxides obtained by the thermal treatment of the HT is found 125 m^2/g.

3.2. Effect of quantity of Mg–Al oxide

The effect of the quantity of Mg–Al oxide on the chloride removal was studied, and the results are shown in Fig. 3. These data have been obtained at initial concentration, temperature, and contact time equal to 99,400 mg/L, 60℃, and 90 min, respectively. It can be observed from Fig. 3(■) that the percentage of chloride removal increased with increasing quantity of Mg–Al oxide.

The Cl^- removal attributed to the rehydration and combination of $Mg_{0.80}Al_{0.20}O_{1.10}$ with Cl^- in wastewater, as shown in Eq. (9):

$$Mg_{0.80}Al_{0.20}O_{1.10} + 0.2Cl^- + 1.1H_2O \rightarrow Mg_{0.80}Al_{0.20}(OH)_2Cl_{0.2} + 0.2OH^- \quad (9)$$

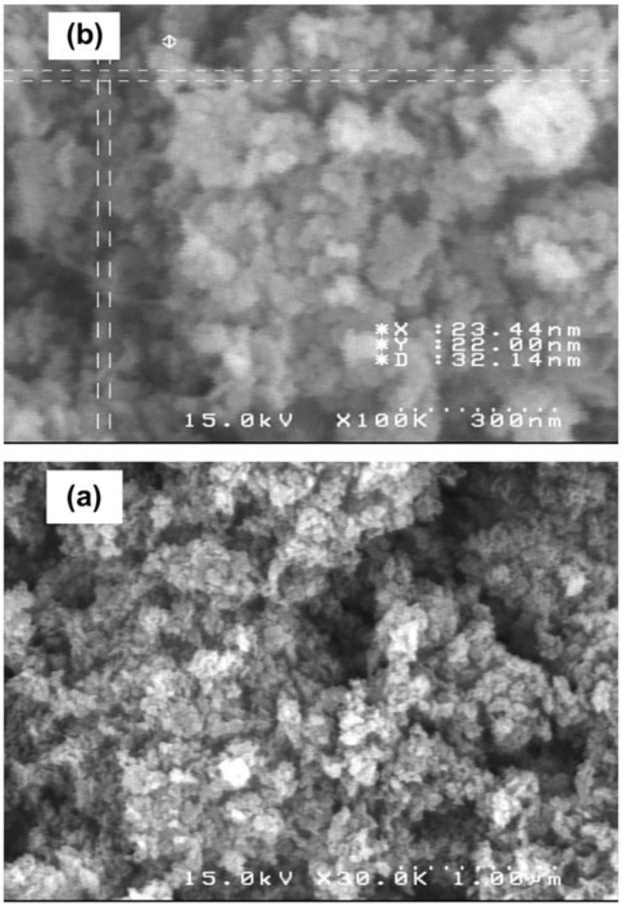

Fig. 2. FESEM micrographs of the nanoparticles and agglomerate Mg–Al oxide (a) relative low magnification and (b) high magnification.

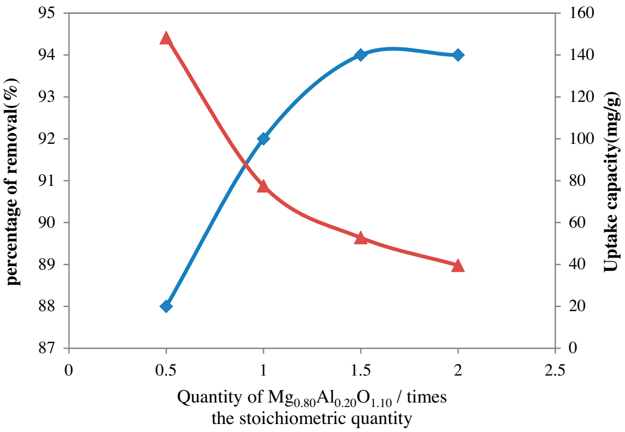

Fig. 3. Relationship between (■) the percentage of chloride removal and (▲) the uptake capacity and the quantity of Mg-Al oxide (C_0 = 99,400 mg/L, T = 60℃, Time = 90 min).

when $Mg_{0.80}Al_{0.20}O_{1.10}$ was added in a stoichiometric quantity according to Eqs. (3)–(5), Cl^- was not removed from the wastewater quantitatively, due to the formation of OH^--HT (HT in which OH^- is the interlayer anion) after the release of OH^-, as expressed in Eq. (10):

$$Mg_{0.80}Al_{0.20}O_{1.10} + 1.1H_2O \rightarrow Mg_{0.80}Al_{0.20}(OH)_2(OH)_{0.2} \quad (10)$$

In this form, the controlling factor depends to the formation of OH^--HT. The increased degree of Cl^- removal is attributed to the higher concentration of Cl^- relative to OH^- in the solution. In general, an anion with a higher charge and a smaller ionic size has a stronger binding affinity to LDHs. For example, the affinity of LDHs for monovalent in organic anions decreases in the order of $OH^- > F^- > Cl^- > Br^- > I^-$ [3]. At 1.5 times, the stoichiometric quantity, more than 93% of the Cl^- was removed from wastewater. More increase in $Mg_{0.80}Al_{0.20}O_{1.10}$ quantity did not have significant effect on removal percentage.

At least 1.5 times of stoichiometric quantity of $Mg_{0.80}Al_{0.20}O_{1.10}$ was found to be required in order to remove Cl^- from solution quantitatively [4]. Therefore, 1.5 times of stoichiometric quantity of Mg–Al oxide have been chosen for further experiments. However, the uptake capacity of $Mg_{0.80}Al_{0.20}O_{1.10}$ decreased upon increasing quantity of $Mg_{0.80}Al_{0.20}O_{1.10}$, as shown in Fig. 3(▲).

3.3. Effect of contact time

The variation of Cl^- removal from wastewater was studied as a function of time. Fig. 4 shows the effect of time on and Cl^- removal by $Mg_{0.80}Al_{0.20}O_{1.10}$ at 30–60˚C. Removal of this ion increased with increasing temperature and time, and reached a maximum value. At 60˚C, the degree of removal increased very rapidly with time, and 94.0% of the Cl^- was removed from wastewater after 0.5 h. At 30˚C, more than 92% of Cl^- was removed after 120 min. This slow reaction suggests that the following two reactions occur: (1) the rehydration and combination of $Mg_{0.80}Al_{0.20}O_{1.10}$ with Cl^- and (2) the anion exchange reaction between Cl^- and OH^- intercalated into the interlayer of OH^--HT formed according to Eq. (10) [27]. As seen from Fig. 4, removal of this ion increases with the increase of temperature. The results indicate that the interaction between chloride and Mg–Al oxide is endothermic in nature. Fig. 5 shows the XRD patterns of the precipitates derived from the reaction of wastewater solution with 1.5 times of stoichiometric quantity of $Mg_{0.80}Al_{0.20}O_{1.10}$. This XRD pattern confirms that $Mg_{0.80}Al_{0.20}O_{1.10}$ converted into HT due to rehydration and combination with anions in aqueous solution.

3.4. Equilibrium isotherms

Equilibrium studies were carried out to determine the optimum conditions for maximum uptake chloride ion by Mg–Al oxide. The equilibrium isotherm is important for describing how the Mg–Al oxide molecules distribute between the liquid and the solid phases when the removal process reaches an equilibrium state. Several models have been published in the literature to describe experimental data of equilibrium isotherms. Two famous isotherm equations, the Langmuir (Eq. (11)) and Freundlich (Eq. (12)) were utilized for further interpretation of the obtained experimental data [4,7,38–40].

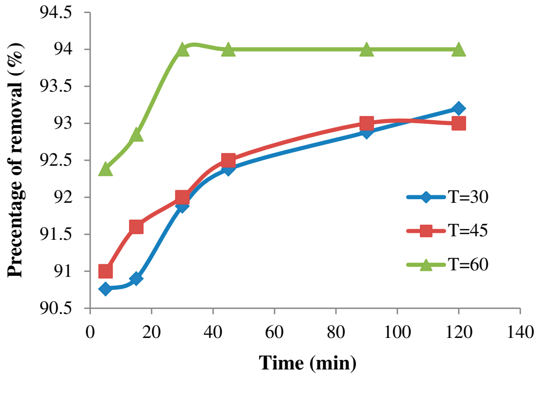

Fig. 4. Effect of contact time on uptake of chloride on Mg–Al oxide.

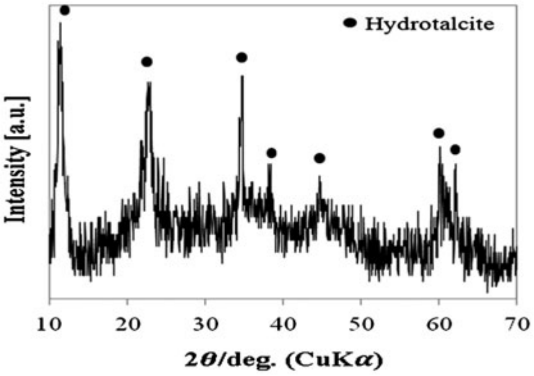

Fig. 5. XRD pattern of precipitates following the reaction of composition of wastewater with 1.5 times the stoichiometric quantity of $Mg_{0.80}Al_{0.20}O_{1.10}$ for 0.5 h.

$$\frac{1}{q_e} = \frac{1}{q_m} + \left(\frac{1}{q_m K_L}\right)\frac{1}{C_e} \tag{11}$$

$$\log q_e = \log K_f + \frac{1}{n}\log C_e \tag{12}$$

where K_L is the Langmuir constant related to the energy of anion exchange; q_m is the maximum uptake capacity; K_f and n are the Freundlich temperature-dependent constants; C_e is the equilibrium concentration of chloride ion in the solution (mg/L); and q_e is the adsorption loading of Mg–Al oxide at equilibrium (mg/g), respectively. Comparison of the equilibrium models, in order to determine which best fitted the experimental results, was performed by linear regression.

The modeling of experimental results by the Langmuir and Freundlich equations are shown in Figs. 6 and 7. The fitted Langmuir parameters (q_m and K_L) and Freundlich constants (K_f and n) and also the correlation coefficient (R^2), are listed in Table 3. The correlation coefficient (R^2) which are reported in Table 3 for both Langmuir and Freundlich isotherm models indicate that both models are able to adequately describe the relationship between q_e and C_e values. However, comparing the results demonstrates that the Langmuir isotherm model fits equilibrium data better than Freundlich model.

The shape of the isotherm may also be considered with a view to predicting if an adsorption process is "favorable" or "unfavorable." The essential characteristics of a Langmuir isotherm can be expressed in terms of a dimensionless separation factor or equilibrium parameter R, which is defined by the following equation [7,38,40]

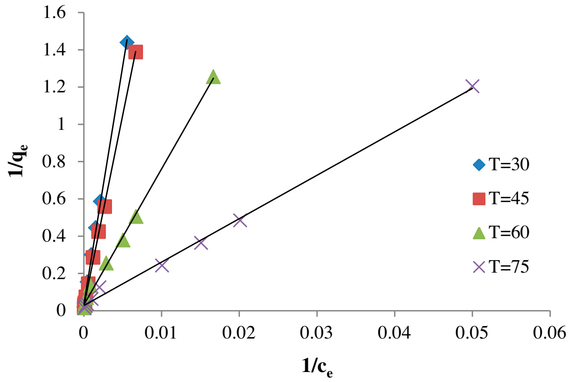

Fig. 6. Langmuir isotherm plots for the chloride anion exchange with Mg–Al oxide at different temperature.

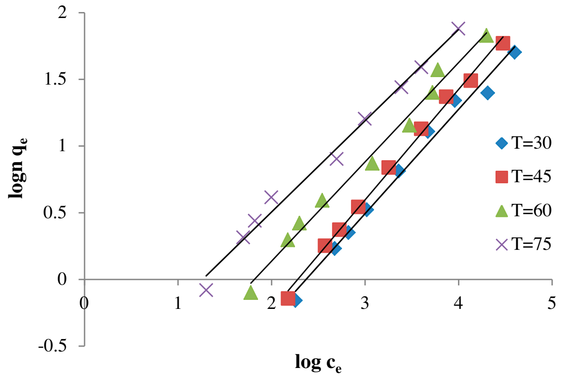

Fig. 7. Freundlich isotherm plots for the chloride anion exchange with Mg–Al oxide at different temperature.

Table 3
Freundlich and Langmuir parameters

	q_m (mg/g)	K_L (L/mg)	R^2
Langmuir isotherm model			
30	29.762	0.000131	0.9986
45	31.847	0.00011	0.9993
60	36.101	0.00043	0.9972
75	44.762	0.001189	0.9966
	n	K_f (L/g)	R^2
Freundlich isotherm model			
30	1.279	0.014077	0.9868
45	1.207	0.01299	0.996
60	1.344	0.04454	0.9890
75	1.462	0.13692	0.9899

$$R = \frac{1}{1 + K_L C_e} \tag{13}$$

According to the value of R the isotherm shape may be interpreted as follows:

- $R > 1$: Unfavorable adsorption process.
- $R = 1$: Linear adsorption process.
- $0 < R < 1$: Favorable adsorption process.
- $R = 0$: Irreversible adsorption process.

The values of R for chloride at 30, 45, 60, and 75°C have been calculated as 0.161–0.977, 0.233–0.984, 0.104–0.975, and 0.078–0.976, respectively. Hence, the process of sorption for chloride removal is favorable.

Thermodynamic parameters such as Gibbs free energy change (ΔG°), enthalpy change (ΔH°), and entropy change (ΔS°) can be estimated by using equilibrium constants changing with temperature. The equilibrium constants obtained from Langmuir model at 30, 45, 60, and 75°C were used to determine the Gibbs free energy changes. From the variations of K_d with temperature, Thermodynamic parameters can be calculated using the following equations [7,39,41]:

$$\text{In}\, K_d = \left(\frac{\Delta S^{\circ}}{R}\right) - \left(\frac{\Delta H^{\circ}}{RT}\right) \tag{14}$$

$$\Delta G^{\circ} = \Delta H^{\circ} - T\Delta S^{\circ} \tag{15}$$

where K_d, ΔH°, ΔS°, R, and T are distribution coefficient (L/g), enthalpy change (J/mol), entropy change (J/mol), universal gas constant (8.314 J/mol K), and temperature (K), respectively. The values of ΔG°, ΔH°, and ΔS° at various temperatures are listed in Table 4. The positive values of ΔG° indicate that the removal process is feasible but not spontaneous for the removal process. The decrease in the value of ΔG° with an increase in temperature indicates that the removal process of chloride become more favorable at higher temperatures [7]. The positive value of ΔH° (45.861 kJ/mol) confirms the endothermic nature of adsorption process, which has been predicted from Fig. 4. The positive value of ΔS° (78.462 J /mol K) suggests the increased randomness at the solid/solution interface for the chloride uptake by Mg–Al oxide [39]. This positive value reflects the affinity of Mg–Al oxide toward chloride ion and suggests some structural change in Mg–Al oxide and chloride ion [7].

3.5. Kinetics of chloride ion removal

Ion exchange experiments carried out in batch mode as a function of time are the most common way to find out the kinetics of the process. In order to clarify the kinetics of chloride ion by Mg–Al oxide, Lagergren's pseudo-first-order and pseudo-second-order kinetic models were applied to the experimental data. The linearized form of the pseudo-first-order rate equation by Lagergren is given as Eq. (16):

$$\ln(q_e - q_t) = \ln q_e - k_1 t \tag{16}$$

Table 4
Gibbs free energy, enthalpy, and entropy changes for the removal of chloride by Mg–Al oxide

Temp. (°C)	ΔG° (kJ/mol)	ΔH° (kJ/mol)	ΔS° (J/mol K)
30	22.087	45.86	78.46
45	20.91		
60	19.73		
75	18.56		

where q_e and q_t are the adsorption loading of chloride (mg/g) at equilibrium and at time t (min), respectively, and k_1 is the rate constant of the equation (min^{-1}) [4,7,38,39,41]. The rate constants (k_1) can be determined experimentally by plotting of $\ln(q_e{-}q_t)$ vs. t. The plots of $\ln(q_e{-}q_t)$ vs. t for the Lagergren-first-order model were not shown as figure because the R^2 values for this model at studied temperatures is low and also the experimental q_e values do not agree with the calculated ones, obtained from the linear plots (Table 5). Experimental data were also applied to the pseudo-second-order kinetic model which is given in the following form: [4,7,38,39,41]

$$\frac{t}{q_t} = \frac{1}{k_2 q_e^2} + \frac{t}{q_e} \tag{17}$$

where k_2 (g/mg min) is the rate constant of the second-order equation. If the second-order kinetics is applicable, then the plot of t/q_t vs. t should show a linear relationship. Values of k_2 and q_e were calculated from the intercept and slope of the plots of t/q_t vs. t. Fig. 8 shows the linear plots of t/q_t vs. t for the pseudo-second-order model for the removal of chloride ion by Mg–Al oxide at 30–60°C. Table 5 shows a good agreement between experimental and calculated q_e values. The correlation coefficients for the second-order kinetic model are greater than 0.996 indicating the applicability of this kinetic equation and the second-order nature of the uptake process of chloride by Mg–Al oxide.

An Arrhenius plot of the adsorption rate against the reciprocal temperature was performed using the kinetic data is shown in Fig. 9, giving a reasonably

Table 5
Pseudo-first-order and second-order rate equation constants for the removal of chloride by Mg–Al oxide at different temperature

	k_1 (min^{-1})	q_e (calculated) (mg/g)	q_e (exp) (mg/g)	R^2
Pseudo-first-order				
30	0.1157	625.03	146.572	0.8033
45	0.1231	31.437	153.312	0.6782
60	0.0172	5.9380	160.551	0.9169
	k_2 (g/ mgmin)	q_e (calculated) (mg/g)	q_e (exp) (mg/g)	R^2
Pseudo-second-order				
30	0.000839	156.25	146.572	0.9963
45	0.0048	153.84	153.312	0.9998
60	0.013255	161.2903	160.551	0.9999

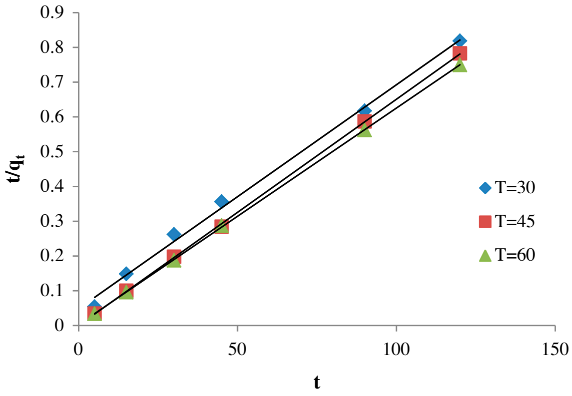

Fig. 8. Second-order kinetic equation for removal of chloride ion by Mg–Al oxide at different temperatures.

straight line ($R^2 = 0.9848$). The gradient of which is (E_a/R) and the activation energy can be calculated according to the well-known Arrhenius expression as Eq. (18):

$$k_2 = Ae^{\left(\frac{-E_a}{RT}\right)} \tag{18}$$

where k_2, A, E_a, R, and T are the rate constant of the pseudo-second-order model (g/mg min), the Arrhenius factor, the activation energy (kJ/mol), the gas constant (8.314 J/mol K), and the temperature (K), respectively. The activation energy could be determined from the slope of the plot of $\ln(k_2)$ vs. $1/T$. The magnitude of activation energy might give an idea about the type of sorption. There are two main types of adsorption: physical and chemical. Activated chemical adsorption means the rate varies with temperature according to finite activation energy (8.4–83.7 kJ/mol) in the Arrhenius equation. In non-activated chemical adsorption, the activation energy is near zero [7].

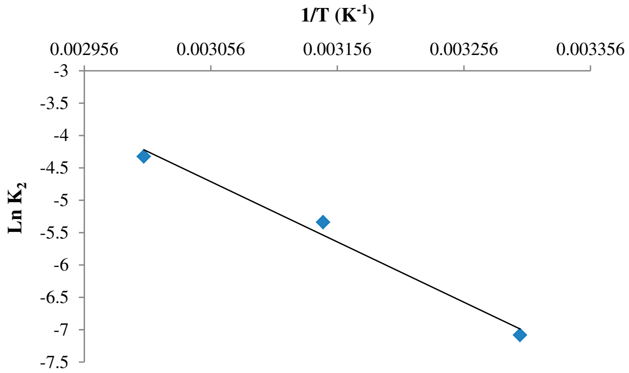

Fig. 9. Arrhenius plot for removal of chloride ion by Mg–Al oxide.

For diffusion-controlled processes, the activation energy of adsorption is <20 kJ/mol. The calculated E_a value is 77.428 kJ/mol, indicates that the process of chloride removal is controlled by the rate of reaction of chloride with the Mg–Al oxide rather than diffusion [4].

4. Conclusion

The efficiency of the Mg–Al oxide, used as anion exchanger to remove chloride ion from aqueous solution has been studied. By increasing $Mg_{0.80}Al_{0.20}O_{1.10}$ quantity, time and temperature, the removal of chloride ion increased. The results showed that 94% of chloride ion from wastewater could be removed within 30 min by using 1.5 times of stoichiometric amount of $Mg_{0.80}Al_{0.20}O_{1.10}$ at 60°C. The structure $Mg_{0.80}Al_{0.20}O_{1.10}$ gradually transforms to LDHs during the process of chloride removal. The equilibrium data were analyzed using the Langmuir and Freundlich isotherm models. Equilibrium data fitted very well with a Langmuir isotherm equation. The pseudo-second-order rate equation described best the kinetic data of chloride ion. The positive values of ΔG° indicate that the uptake process is feasible but not spontaneous; the positive value of ΔH° confirms the endothermic nature of adsorption; and the positive value of ΔS° suggests the increased randomness at the solid/solution interface for the chloride uptake by Mg–Al oxide. Finally, the results showed that proposed method can be utilized for wastewater treatment with high amount of inorganic matters, especially those that are produced in sodium carbonate production industries.

References

[1] Y. Horii, S. Higuchi, T. Shimaoka, M. Hanashima, The treatment technology of landfill leachates containing condensed inorganic salts, Waste Manage. Res. 8 (1997) 529–539.
[2] T. Kameda, F. Yabuuchi, T. Yoshioka, M. Uchida, A. Okuwaki, New method of treating dilute mineral acids using magnesium–aluminum oxide, Water Res. 37 (2003) 1545–1550.
[3] T. Kameda, T. Yoshioka, T. Mitsuhashi, M. Uchida, A. Okuwaki, The simultaneous removal of calcium and chloride ions from calcium chloride solution using magnesium–aluminum oxide, Water Res. 37 (2003) 4045–4050.
[4] L. Lv, J. He, M. Wei, D.G. Evans, X. Duan, Uptake of chloride ion from aqueous solution by calcined layered double hydroxides: Equilibrium and kinetic studies, Water Res. 40 (2006) 735–743.

[5] T. Kameda, Y. Miyano, T. Yoshioka, M. Uchida, A. Okuwaki, New treatment methods for waste water containing chloride lon using magnesium–aluminum oxide, Chem. Lett. 29 (2000) 1136–1137.

[6] A.D. Eaton, M.A.H. Franson, A.P.H. Association, A.W.W. Association, W.E. Federation, Standard Methods for the Examination of Water and Wastewater, American Public Health Association, Washington, DC, 2005.

[7] Y. Yao, F. Xu, M. Chen, Z. Xu, Z. Zhu, Adsorption behavior of methylene blue on carbon nanotubes, Bioresour. Technol. 101 (2010) 3040–3046.

[8] T. Kasikowski, R. Buczkowski, E. Lemanowska, Cleaner production in the ammonia–soda industry: An ecological and economic study, J. Environ. Manage. 73 (2004) 339–356.

[9] C. Gao, Y. Dong, H. Zhang, J. Zhang, Utilization of distiller waste and residual mother liquor to prepare precipitated calcium carbonate, J. Clean. Prod. 15 (2007) 1419–1425.

[10] T. Kasikowski, R. Buczkowski, B. Dejewska, K. Peszyńska-Białczyk, E. Lemanowska, B. Igliński, Utilization of distiller waste from ammonia–soda processing, J. Clean. Prod. 12 (2004) 759–769.

[11] T. Kasikowski, R. Buczkowski, M. Cichosz, Utilisation of synthetic soda-ash industry by-products, Int. J. Prod. Econ. 112 (2008) 971–984.

[12] S. Miyata, Anion-exchange properties of hydrotalcite-like compounds, Clays Clay Miner. 31 (1983) 305–311.

[13] R. Allmann, The crystal structure of pyroaurite, Acta Crystallogr., Sect. B: Struct. Crystallogr. Cryst. Chem. 24 (1968) 972–977.

[14] T. Sato, T. Wakabayashi, M. Shimada, Adsorption of various anions by magnesium aluminum oxide of ($Mg_{0.7}Al_{0.3}O_{1.15}$), Ind. Eng. Chem. Prod. Res. Dev. 25 (1986) 89–92.

[15] T. Sato, M. Tezuka, T. Endo, M. Shimada, Kinetics of anion uptake by rock salt-type magnesium aluminium oxide solid solutions, React. Solids 3 (1987) 287–295.

[16] S. Miyata, Physico-chemical properties of synthetic hydrotalcites in relation to composition, Clays Clay Miner. 28 (1980) 50–56.

[17] M.Z.B. Hussein, Z. Zainal, I. Yaziz, T.C. Beng, The use of Mg/Al layered double hydroxide for color removal of textile wastewater, J. Environ. Sci. Health. Part A: Toxic/Hazard. Subst. Environ. Eng, 36 (2001) 565–573.

[18] C. Díaz-Nava, M. Solache-Ríos, M.T. Olguín, Sorption of fluoride ions from aqueous solutions and well drinking water by thermally treated hydrotalcite, Sep. Sci. Technol. 38 (2003) 131–147.

[19] M.C. Hermosín, I. Pavlovic, M.A. Ulibarri, J. Cornejo, Trichlorophenol adsorption on layered double hydroxide: A potential sorbent, J. Environ. Sci. Health., Part A Environ. Sci. Eng. Toxic Hazard. Subst. Control 28 (1993) 1875–1888.

[20] L.P. Cardoso, J. Tronto, E.L. Crepaldi, J.B. Valim, Removal of benzoate anions from aqueous solution using Mg–Al layered double hydroxides, Mol. Cryst. Liq. Cryst. 390 (2003) 49–56.

[21] F. Kooli, I.C. Chisem, M. Vucelic, W. Jones, Synthesis and properties of terephthalate and benzoate intercalates of Mg−Al layered double hydroxides possessing varying layer charge, Chem. Mater. 8 (1996) 1969–1977.

[22] S.-L. Wang, C.-Y. Cheng, Y.-M. Tzou, R.-B. Liaw, T.-W. Chang, J.-H. Chen, Phosphate removal from water using lithium intercalated gibbsite, J. Hazard. Mater. 147 (2007) 205–212.

[23] Y. Seida, Y. Nakano, Removal of phosphate by layered double hydroxides containing iron, Water Res. 36 (2002) 1306–1312.

[24] R.L. Goswamee, P. Sengupta, K.G. Bhattacharyya, D.K. Dutta, Adsorption of Cr(VI) in layered double hydroxides, Appl. Clay Sci. 13 (1998) 21–34.

[25] Y.-M. Tzou, S.-L. Wang, L.-C. Hsu, R.-R. Chang, C. Lin, Deintercalation of Li/Al LDH and its application to recover adsorbed chromate from used adsorbent, Appl. Clay Sci. 37 (2007) 107–114.

[26] S.V. Prasanna, P. Vishnu Kamath, Chromate uptake characteristics of the pristine layered double hydroxides of Mg with Al, Solid State Sci. 10 (2008) 260–266.

[27] T. Kameda, T. Yoshioka, M. Uchida, Y. Miyano, A. Okuwaki, New treatment method for dilute hydrochloric acid using magnesium–aluminum oxide, Bull. Chem. Soc. Jpn. 75 (2002) 595–599.

[28] T. Kameda, T. Yoshioka, T. Hoshi, M. Uchida, A. Okuwaki, The removal of chloride from solutions with various cations using magnesium–aluminum oxide, Sep. Purif. Technol. 42 (2005) 25–29.

[29] T. Kameda, N. Uchiyama, K.-S. Park, G. Grause, T. Yoshioka, Removal of hydrogen chloride from gaseous streams using magnesium–aluminum oxide, Chemosphere 73 (2008) 844–847.

[30] T. Kameda, N. Uchiyama, T. Yoshioka, Treatment of gaseous hydrochloric acid with magnesium–aluminum oxide using batch operation, Desalination 280 (2011) 424–427.

[31] T. Kameda, T. Yoshioka, T. Hoshi, M. Uchida, A. Okuwaki, Treatment of hydrochloric acid with magnesium–aluminum oxide at ambient temperatures, Sep. Purif. Technol. 51 (2006) 272–276.

[32] T. Kameda, M. Nakamura, T. Yoshioka, Removal of antimonate ions from an aqueous solution by anion exchange with magnesium–aluminum layered double hydroxide and the formation of a brandholzite-like structure, J. Environ. Sci. Health., Part A: Toxic/Hazard. Subst. Environ. Eng, 47 (2012) 1146–1151.

[33] Y.W. You, H.T. Zhao, G.F. Vance, Removal of arsenite from aqueous solutions by anionic clays, Environ. Technol. 22 (2001) 1447–1457.

[34] F. Cavani, F. Trifirò, A. Vaccari, Hydrotalcite-type anionic clays: Preparation, properties and applications, Catal. Today 11 (1991) 173–301.

[35] J. He, M. Wei, B. Li, Y. Kang, D. Evans, X. Duan, Preparation of layered double hydroxides, in: X. Duan, D. Evans (Eds.), Layered Double Hydroxides. Springer Berlin Heidelberg, Berlin, 2006, pp. 89–119.

[36] R. Hamidi, D. Kahforoushan, E. Fatehifar, The simultaneous removal of calcium, magnesium and chloride ions from industrial wastewater using magnesium–aluminum oxide, J. Environ. Sci. Health. Part A 48 (2013) 1225–1230.

[37] P. Kuśtrowski, D. Sułkowska, L. Chmielarz, A. Rafalska-Łasocha, B. Dudek, R. Dziembaj, Influence of thermal treatment conditions on the activity of hydrotalcite-derived Mg–Al oxides in the aldol condensation of acetone, Microporous Mesoporous Mater. 78 (2005) 11–22.

[38] O. Hamdaoui, Batch study of liquid-phase adsorption of methylene blue using cedar sawdust and crushed brick, J. Hazard. Mater. 135 (2006) 264–273.

[39] L. Lv, P. Sun, Z. Gu, H. Du, X. Pang, X. Tao, R. Xu, L. Xu, Removal of chloride ion from aqueous solution by ZnAl–NO_3 layered double hydroxides as anion-exchanger, J. Hazard. Mater. 161 (2009) 1444–1449.

[40] M. Doğan, M. Alkan, Removal of methyl violet from aqueous solution by perlite, J. Colloid Interface Sci. 267 (2003) 32–41.

[41] A. Sarı, M. Tuzen, D. Cıtak, M. Soylak, Adsorption characteristics of Cu(II) and Pb(II) onto expanded perlite from aqueous solution, J. Colloid Interface Sci. 148 (2007) 387–394.